2020 IEEE 17th International Symposium on Biomedical Imaging (ISBI)
April 3-7, 2020, Iowa City, Iowa, USA

AUTOMATIC CLASSIFICATION OF ARTERY/VEIN FROM SINGLE WAVELENGTH FUNDUS IMAGES

P. Kevin Raj[1], *Aniketh Manjunath*[2], *J. R. Harish Kumar*[1,3] *and Chandra Sekhar Seelamantula*[1]

[1]Department of Electrical Engineering, Indian Institute of Science, Bangalore, India
[2]Department of Computer Science, USC Viterbi School of Engineering, California, USA
[3]Department of Electrical and Electronics Engineering, MIT, MAHE, Manipal, India
anikethm@usc.edu, {kevinraj, harishj, css}@iisc.ac.in

ABSTRACT

Vessels are regions of prominent interest in retinal fundus images. Classification of vessels into arteries and veins can be used to assess the oxygen saturation level, which is one of the indicators for the risk of stroke, condition of diabetic retinopathy, and hypertension. In practice, dual-wavelength images are obtained to emphasize arteries and veins separately. In this paper, we propose an automated technique for the classification of arteries and veins from single-wavelength fundus images using convolutional neural networks employing the ResNet-50 backbone and squeeze-excite blocks. We formulate the artery-vein identification problem as a three-class classification problem where each pixel is labeled as belonging to an artery, vein, or the background. The proposed method is trained on publicly available fundus image datasets, namely RITE, LES-AV, IOSTAR, and cross-validated on the HRF dataset. The standard performance metrics, such as average sensitivity, specificity, accuracy, and area under the curve for the datasets mentioned above, are 92.8%, 93.4%, 93.4%, and 97.5%, respectively, which are superior to the state-of-the-art methods.

Index Terms— Artery-vein (A/V), classification, convolutional neural network (CNN), fundus images.

1. INTRODUCTION

Retinal oximetry is a non-invasive imaging technique used to measure the retinal oxygen saturation level using multi-wavelength fundus images, which is used to address the problem of retinal vessel occlusion, diabetic retinopathy, and hypertension. The above mentioned pathologies alter the topography of blood vessels in the retina and lower the arteriolar-to-venular ratio (AVR), indicating that the patient is suffering from the risk of hypertension and cardiovascular diseases [1]. This methodology is expensive and time-consuming compared to traditional fundus imaging in which one captures a single-wavelength fundus image. Hence, there is a need to investigate the possibility of artery-vein (A/V) classification using single-wavelength fundus image (Fig. 1). There have been numerous image processing techniques as well as deep learning approaches reported in the literature that address A/V classification. On the image processing front, Behdad et al. extracted the graph of vasculature and used intensity features to identify whether the vessel pixel is an artery or a vein [2]. Similarly, in [3], [4], the authors used a graph of the vasculature to estimate the topological and geometrical features to improve A/V classification performance. Qazaleh et al.'s methodology consists of three parts: pre-processing, feature extraction along the vessel centerline, and post-processing techniques for the classification of vessels into arteries or veins [5]. On the deep learning front, A/V classification is done with the help of features extracted using a fully connected convolutional neural network [6], [7], and uncertainty-based classification using U-Net architecture proposed by [8]. Recently, Zhang et al. proposed a cascaded refined U-net based A/V classification using dual-modal fundus images consisting of two monochromatic images captured at wavelengths 570 and 610 nm [9].

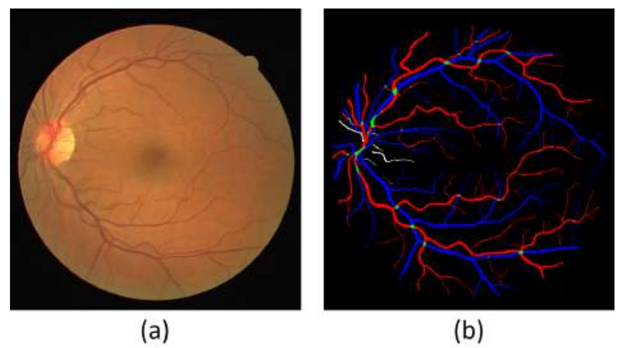

Fig. 1. [Color online] (a) A color fundus image; (b) Manual annotation: red indicates artery, blue indicates vein, green indicates overlapping of arteries and veins, and white indicates neither artery nor vein.

This work was supported by the Ministry of Human Resource Development under the IMPRINT India Initiative (Domain: Healthcare; Project No.: 6013).

Authorized licensed use limited to: Max-Planck-Institut fuer Informatik . Downloaded on November 15,2023 at 12:54:40 UTC from IEEE Xplore. Restrictions apply.

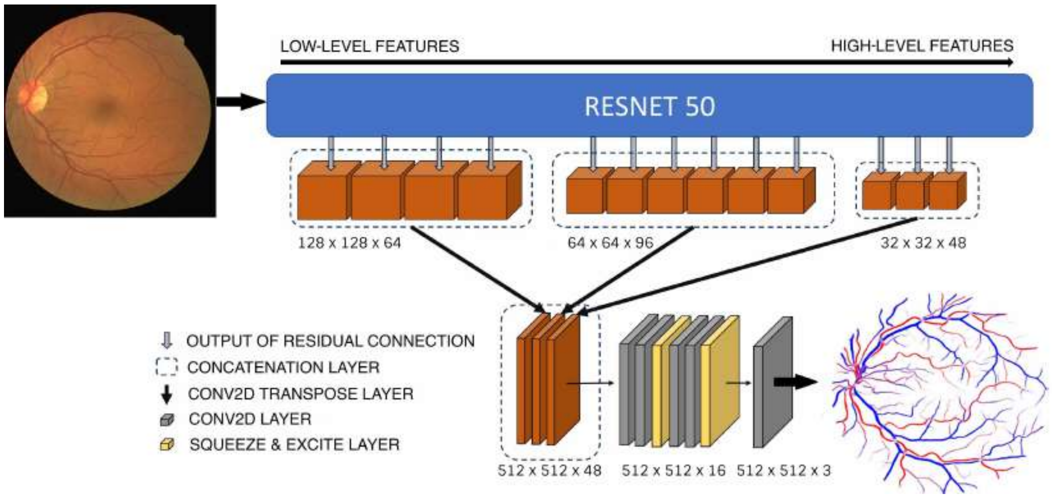

Fig. 2. [Color online] Proposed AV-Net for artery/vein classification.

1.1. Our Contribution

Our main contribution in this paper is a novel CNN architecture for A/V classification using ResNet-50 backbone and *Squeeze-Excite* blocks. In contrast to the other methods, a segmented vasculature map is not required as the input to the A/V classification network. The network only requires a single wavelength, color fundus image as the input. The proposed CNN is extensively validated on three publicly available datasets and also cross-validated on an unseen dataset. The results indicate the superior generalization capability of the network.

2. PROPOSED METHOD

The proposed technique performs pixel-level classification of the fundus image into arteries/veins without the need for preprocessing of fundus images or a segmented vasculature map. As the depth of the network increases, the network is prone to vanishing/exploding gradients. To address this problem, He et al. introduced residual connections [10]. We propose a novel network named AV-Net by combining the low-level to high-level features extracted from the residual connections of ResNet-50. We have incorporated *Squeeze-Excite* networks [11] and recently developed rectified Adam optimizer [12] to optimize the proposed architecture.

2.1. Artery-Vein Net (AV-Net)

We use ResNet-50 [10], as the backbone network to perform feature extraction. The ResNet-50 is pre-trained on the ImageNet dataset [13]. The residual blocks separate the ResNet-50 architecture into 16 sub-blocks, each consisting of several convolutions, activation, and batch normalization operations. We concatenate the features extracted from the residual blocks having the same filter dimensions. The extracted features are upsampled to match the output dimension of 512×512. The upsampled features are then concatenated and passed to squeeze and excite blocks, to explicitly model the inter-dependencies between various channels. A block diagram of the proposed architecture is shown in Fig. 2.

Table 1. Overview of datasets used for A/V classification.

Dataset	# images	Resolution
RITE [14]	40	565×584
LES-AV [15]	22	1444×1620
IOSTAR [16]	30	1024×1024
HRF [17]	45	3504×2336

2.2. Training

The AV-Net is trained for 30 epochs with a batch size of two images in order to minimize the three-class categorical cross-entropy ($\mathcal{CCE}$) loss function:

$$\mathcal{CCE} = -\sum_{c=0}^{2} y_c \log\left(\frac{e^{\hat{y}_c}}{\sum_{i=0}^{2} e^{\hat{y}_i}}\right), \tag{1}$$

where y_c indicates the correct label and $\hat{y}_c$ indicates the predicted probability of a pixel being an artery, vein, or the background class ($c, i \in [0, 2]$), respectively. The loss function is optimized by using rectified Adam [12], which uses warm-up, an initial period of training with a much lower learning rate so that adaptive optimizers can offset excessive variance when dealing with limited training data. The optimal learning rate $7e-3$ for the optimizer is obtained using a grid search.

Authorized licensed use limited to: Max-Planck-Institut fuer Informatik . Downloaded on November 15,2023 at 12:54:40 UTC from IEEE Xplore. Restrictions apply.

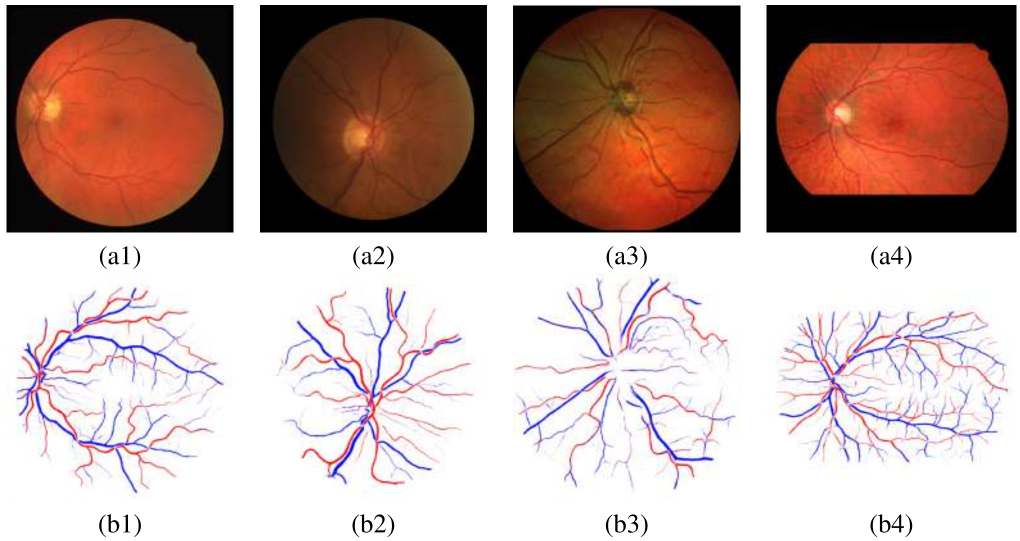

Fig. 3. [Color online] Extraction of artery-vein vasculature using AV-Net. (a1)-(a4): Fundus images; (b1)-(b4): Results on images from (b1) RITE, (b2) LES-AV, (b3) IOSTAR, and (b4) HRF datasets (blue indicates vein and red indicates artery).

3. EXPERIMENTAL VALIDATION

The AV-Net is trained on three different publicly available datasets namely: RITE [14], IOSTAR [16], LES-AV [15], and cross-validated on HRF [17]. These datasets contain images of different contrast, brightness, and illumination, as shown in Fig. 3. An overview of the datasets mentioned above is given in Table 1. Unlike the other datasets, INSPIRE [2] provides only center-line annotation. Hence, we have opted not to include INSPIRE in our study. In the case of RITE and HRF datasets, ground truth was labeled as neither an artery nor a vein inside the optic disc region and in crossings between vessels. We have not considered these miscellaneous cases to enable objective comparisons with the previously proposed methods, which considered A/V classification as a binary classification problem, i.e., classifying into either an artery or a vein. A total of 92 images obtained from RITE, IOSTAR, and LES-AV datasets are distributed randomly into training and validation sets (70% & 30%, respectively). Data augmentation techniques such as rotation, shearing, horizontal, and vertical flip have been employed to increase the size of the training data. Finally, the input images are resized to 1024×1024 and fed as the input to the network without any pre-processing. Manual annotations of A/V are resized to 512×512 to match the output dimensions of the network. Metrics such as sensitivity (S_n), specificity (S_p), accuracy (A_c), and area under the curve (AUC) are reported for the combined train-test set in Table 2. To assess the generalization of the AV-Net, we have also reported cross-validation scores on the HRF dataset. ROC analysis is performed separately for both artery and vein, to choose the optimal threshold value that maximizes the Youden index $J = S_n + S_p - 1$. Techniques [8, 18, 19] generate pixel-wise A/V classification map and do not require a segmented vasculature map, whereas [20–22] require a binary vessel map as an input and it is obtained by their proposed techniques. An extensive comparison of the proposed technique with state-of-the-art techniques is shown in Table 2.

Table 2. Comparison of AV-Net with state-of-the-art techniques.

Dataset	Method	Vessel map required as input	S_n	S_p	A_c	AUC
HRF	FCN [18]	✓	-	-	**0.965**	-
	AV-NET	✗	**0.907**	**0.915**	0.915	**0.965**
IOSTAR	**AV-NET**	✗	**0.925**	**0.932**	**0.932**	**0.975**
LES-AV	UV-AV [8]	✗	0.88	0.85	0.86	0.94
	AV-NET	✗	**0.944**	**0.946**	**0.946**	**0.98**
RITE	FCN [18]	✗	-	-	0.938	-
	UV-AV [8]	✗	0.89	0.9	0.89	0.95
	DS-UNET [19]	✗	0.923	0.911	0.917	-
	DFS-search + RF [20]	✓	**0.94**	0.939	0.939	-
	GrBs [2]	✓	0.9	0.84	0.85	-
	TpEs [21]	✓	0.917	0.917	0.92	-
	GenS [22]	✓	0.71	0.74	0.72	0.78
	AV-NET	✗	0.937	**0.943**	**0.943**	**0.98**

4. CONCLUSION

We have proposed a novel deep learning architecture named AV-Net for artery/vein classification from a single wavelength fundus image using low-level to high-level features extracted from residual connections of ResNet-50. In contrast with previously proposed techniques, AV-Net does not require a segmented vasculature map as the input. The network is extensively validated on publicly available datasets RITE, IOSTAR, LES-AV, and cross-validated on HRF, indicating efficacy and generalization capability of AV-Net.

Authorized licensed use limited to: Max-Planck-Institut fuer Informatik . Downloaded on November 15,2023 at 12:54:40 UTC from IEEE Xplore. Restrictions apply.

5. REFERENCES

[1] M. K. Ikram et al., "Are retinal arteriolar or venular diameters associated with markers for cardiovascular disorders? The Rotterdam study," *Investigative Ophthalmology & Visual Science*, vol. 45, no. 7, pp. 2129–2134, 2004.

[2] B. Dashtbozorg, A. M. Mendonça, and A. Campilho, "An automatic graph-based approach for artery/vein classification in retinal images," *IEEE Transactions on Image Processing*, vol. 23, no. 3, pp. 1073–1083, 2013.

[3] M. E. Martinez-Perez et al., "Retinal vascular tree morphology: A semi-automatic quantification," *IEEE Transactions on Biomedical Engineering*, vol. 49, no. 8, pp. 912–917, 2002.

[4] Y. Zhao et al., "Retinal artery and vein classification via dominant sets clustering-based vascular topology estimation," in *Proc. Int. Conf. on MICCAI*, 2018, pp. 56–64.

[5] Q. Mirsharif, F. Tajeripour, and H. Pourreza, "Automated characterization of blood vessels as arteries and veins in retinal images," *Computerized Medical Imaging and Graphics*, vol. 37, no. 7-8, pp. 607–617, 2013.

[6] M. I. Meyer et al., "Deep convolutional artery/vein classification of retinal vessels," in *Proc. Int. Conf. on Image Analysis and Recognition*, 2018, pp. 622–630.

[7] R. A. Welikala et al., "Automated arteriole and venule classification using deep learning for retinal images from the U.K. Biobank cohort," *Computers in Biology and Medicine*, vol. 90, pp. 23–32, 2017.

[8] A. Galdran et al., "Uncertainty-aware artery/vein classification on retinal images," in *Proc. IEEE Int. Symp. on Biomed. Imag.*, 2019, pp. 556–560.

[9] S. Zhang et al., "Simultaneous arteriole and venule segmentation of dual-modal fundus images using a multi-task cascade network," *IEEE Access*, vol. 7, pp. 57561–57573, 2019.

[10] K. He, X. Zhang, S. Ren, and J. Sun, "Deep residual learning for image recognition," in *Proc. IEEE Int. Conf. on CVPR*, 2016, pp. 770–778.

[11] J. Hu, L. Shen, and G. Sun, "Squeeze-and-excitation networks," in *Proc. IEEE Int. Conf. on CVPR*, 2018, pp. 7132–7141.

[12] L. Liu et al., "On the variance of the adaptive learning rate and beyond," *arXiv preprint arXiv:1908.03265*, 2019.

[13] J. Deng et al., "Image Net: A large-scale hierarchical image database," in *Proc. IEEE Int. Conf. on CVPR*, 2009, pp. 248–255.

[14] Q. Hu, M. D. Abràmoff, and M. K. Garvin, "Automated separation of binary overlapping trees in low-contrast color retinal images," in *Proc. Int. Conf. on MICCAI*. Springer, 2013, pp. 436–443.

[15] J. I. Orlando et al., "Towards a glaucoma risk index based on simulated hemodynamics from fundus images," in *Proc. Int. Conf. on MICCAI*, 2018, pp. 65–73.

[16] S. A. Sureshjani, I. Smit-Ockeloen, J. Zhang, and B. T. H. Romeny, "Biologically-inspired supervised vasculature segmentation in slo retinal fundus images," in *Proc. Int. Conf. on Image Analysis and Recognition*, 2015, pp. 325–334.

[17] J. Odstrcilik et al., "Retinal vessel segmentation by improved matched filtering: evaluation on a new high-resolution fundus image database," *IET Image Processing*, vol. 7, no. 4, pp. 373–383, 2013.

[18] R. Hemelings et al., "Artery-vein segmentation in fundus images using a fully convolutional network," *Computerized Medical Imaging and Graphics*, 2019.

[19] Z. Wang, J. Lin, R. Wang, and W. Zheng, "Retinal artery/vein classification via rotation augmentation and deeply supervised U-net segmentation," in *Proc. Int. Conf. on Biomedical Signal and Image Processing*, 2019, pp. 71–76.

[20] C. L. Srinidhi, P. Aparna, and J. Rajan, "Automated method for retinal artery/vein separation via graph search metaheuristic approach," *IEEE Transactions on Image Processing*, vol. 28, no. 6, pp. 2705–2718, 2019.

[21] R. Estrada et al., "Retinal artery-vein classification via topology estimation," *IEEE Transactions on Medical Imaging*, vol. 34, no. 12, pp. 2518–2534, 2015.

[22] F. Huang, B. Dashtbozorg, T. Tan, and B. M. T. Romeny, "Retinal artery/vein classification using genetic-search feature selection," *Computer Methods and Programs in Biomedicine*, vol. 161, pp. 197–207, 2018.

Authorized licensed use limited to: Max-Planck-Institut fuer Informatik . Downloaded on November 15,2023 at 12:54:40 UTC from IEEE Xplore. Restrictions apply.